Microstructural Evolution and Mechanical Anisotropy of AA6061 Fabricated by Additive Friction Stir Deposition

U. Ashok Kumar[1*], Harshith Karanam[2], MVS Vamsy Krishna[3], Sohail Shaik[4]

[1,2,3,4] Department of Mechanical Engineering, University College of Engineering (A), Osmania University, Hyderabad, INDIA

uak.oumech@gmail.com, harshithk.be26@uceou.edu, vamsykrishnamanem108@gmail.com, skanime987@gmail.com

Abstract. The growing demand for lightweight, high-performance structural components has increased interest in solid-state additive manufacturing methods for aluminum alloys. Additive Friction Stir Deposition (FSD) is a solid-state process that builds material layer by layer through severe plastic deformation and frictional heating without melting, thereby reducing porosity, residual stresses, and solidification-related defects common in fusion-based techniques. In this study, AA6061 alloy was fabricated using AFSD at traverse speeds of 250, 300, and 350 mm/min with tool rotational speeds of 900, 1120, and 1400 rpm to evaluate the influence of processing parameters on mechanical and micro structural behavior. The deposits were characterized using tensile testing, Vickers microhardness measurements, pin-on-disc wear testing, and optical microscopy in both as-deposited and heat-treated conditions. Microstructural analysis revealed refined equiaxed grains and strong interlayer bonding, demonstrating that AFSD can provide competitive mechanical performance with enhanced ductility and structural integrity

Keywords: AA6061; Additive Friction Stir Deposition; Heat Treatment; Mechanical Properties; Microstructure.

1 INTRODUCTION

The rising need for lightweight yet strong materials has boosted the use of aluminium alloys in transportation, aerospace, and automotive industries. Their favourable strength-to-weight ratio makes them a popular choice for creating efficient structural parts. However, traditional fusion-based joining and manufacturing methods often cause problems like porosity, segregation, and cracking, limiting the reliability of these alloys in critical applications [1][2].To tackle these issues, new solid-state methods have been developed. One of these is friction stir welding (FSW), known for creating defect-free joints by skipping the melting phase and using mechanical stirring along with localized heat [8]. This method has evolved into friction stir additive manufacturing (AFSD), a new technique where materials are built up layer by layer in

S. Uppapalli and D. Chakraborty (eds.), *Proceedings of the International Conference on Mechanics, Materials and Mechatronics (ICM³ 2026)*, Atlantis Highlights in Engineering 47,
https://doi.org/10.2991/978-94-6239-764-4_11

solid form [3]. AFSD allows for the production of near-net-shape components while reducing defects commonly tied to fusion-based additive manufacturing methods [4]. Additive manufacturing (AM) as a broader field has been adopted in various industries for its ability to produce customized and complex geometries. Comprehensive reviews highlight how AM encompasses a range of processes, including powder-bed fusion, directed energy deposition, and newer solid-state approaches such as AFSD [5].Alongside these advancements, beam-based additive manufacturing, such as selective laser melting (SLM), has also been studied extensively. SLM can create complex shapes with precision; however, it still faces challenges like high residual stresses, anisotropy, and process-induced porosity [6][7].These issues have pointed to the need for alternative methods, and AFSD is becoming a strong contender, especially for aluminium alloys [3][8].Recent studies have examined the microstructure and mechanical properties of additively manufactured aluminium alloys using both AFSD and SLM. For instance, research on AlSi10Mg alloys made with SLM showed high hardness but also revealed flaws from the process that impact long-term durability [6][7]. In contrast, AFSD studies on Al6061 and similar alloys have shown better microstructures and increased hardness across build layers, proving that this process can deliver consistent performance in multilayer builds [4][8][2]. In this context, the current work evaluates the potential of AFSD for producing aluminium alloy structures and compares its performance with both standard aluminium and SLM-produced options. Specifically, three AFSD samples were made under different process conditions. Each sample underwent mechanical testing and microstructural analysis, and the best-performing sample was chosen as a benchmark. Finally, to enhance the practical relevance of the study, a real-world component was designed using the properties of the optimal sample, and its performance was compared to the same part made using traditional methods and SLM. This approach offers both experimental insights and validation of AFSD as a competitive method for making lightweight structural components.

2 LITERATURE REVIEW

The demand for lightweight structural components with improved strength-to-weight ratios has sped up the development of solid-state joining and additive processes. Conventional fusion-based methods for aluminium alloys often lead to defects such as porosity, cracking, and segregation. These defects limit their use in high-performance sectors [1]. To address these issues, friction stir welding (FSW) was introduced. This solid-state technique uses a rotating non-consumable tool to plastically deform and join materials without melting. Its success in welding aluminium alloys paved the way for friction stir additive manufacturing [2]. Recent studies show FSAM as a good method for making layered structures with few defects. Mishra (2022) described FSAM as an extension of FSW that facilitates the production of multilayer metallic components with strong structural integrity and reduced need for post-processing [3]. Gao (2025) explored the microstructure of Al 6061 builds created through additive friction stir deposition. His work confirmed that FSAM can refine grains and increase hardness while lowering porosity compared to traditional casting [4]. Optimization studies also stressed the importance of process parameters. A screening study on different aluminium alloys demonstrated how tool rotation speed and traverse rate directly influence the tensile strength and hardness of FSAM builds. This finding highlights the necessity for careful parameter control to achieve defect-free parts [8]. Elangovan (2008) supported this by experimentally showing that changes in tool pin profile and welding speed affect the microstructure and hardness of Al6061 joints [2]. In contrast, beam-based additive methods like Selective Laser Melting (SLM) are also widely researched. Zhang (2019) analyzed AlSi10Mg parts made through SLM and noted their superior tensile strength, along with challenges such as brittleness and surface finish [6]. Similarly, N. Read (2015) pointed out process optimization strategies for SLM to enhance the mechanical properties of Al-Si10Mg alloys but identified ongoing issues with porosity and cracking in fusion-based methods [7]. When comparing AFSD to SLM, these findings suggest that while SLM excels in strength, AFSD provides better ductility and structural reliability. From a broader perspective, Gibson (2015) classified FSAM within the larger set of additive manufacturing technologies, noting its energy efficiency, reduced material waste, and potential for scaling up in industrial applications [5]. These benefits make AFSD particularly appealing for aerospace and automotive industries, where sustainable manufacturing and high-performance alloys are increasingly necessary. Despite these advances, there is a gap in direct comparisons of FSAM builds with both traditional and SLM-produced parts tested under the same conditions. Most studies focus on microstructural evaluation, parameter analysis, or optimization separately [3][4][6]. Khodabakshi and gerlich (2018),Yu and Mishra (2020) highlighted its ability to produce dense components with refined grain structures and low residual stresses and improved the mechanical properties compared with fusion based additive manufacturing [9] [10] [11] [12]. Similarly Perry (2020),Phillips (2019) and Zeng (2022) demonstrated that dynamic recrystallization during AFSD enchnces interlayer bonding ,hardness and tensile performance of AA606 alloys [13] [14][15].The current research aims to fill this gap by experimentally fabricating three FSAM –stir Deposition type samples of AA6061. It analyzes their tensile strength, hardness, wear, and microstructural performance to identify the best-performing sample. This sample is further compared to conventional and SLM-produced parts to assess AFSD’s viability as a practical manufacturing option.

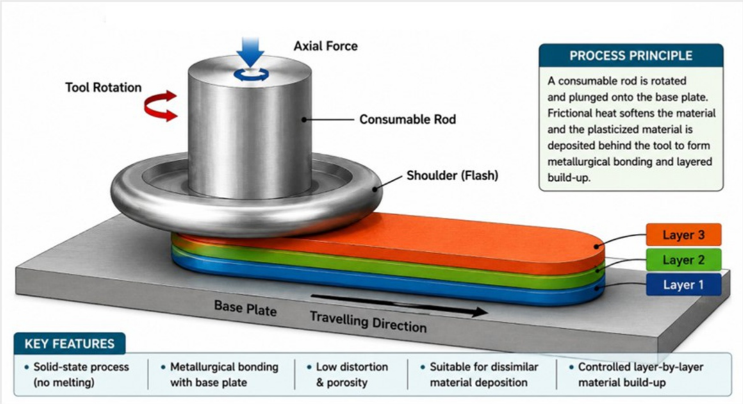

Fig. 1. Additive Friction Stir Deposition

3 EXPERIMENTAL METHODOLOGY

3.1 Material Fabrication by AFSD

The current study used AA6061 alloy as the feed material because it is commonly employed in aerospace, automotive, and marine sectors. A mild steel (MS) plate, measuring 120 mm × 120 mm, served as the base support to ensure rigidity and stability during the deposition process. All depositions took place on a vertical milling machine, specifically modified for AFSD fig.2. This modification involved strengthening the spindle and fixture setup to withstand the axial and transverse forces created during the process. The AA6061 was chosen with a shoulder diameter of around 18 mm, and a length of 100 mm. Three multi-layered samples were created, each containing three deposited layers. The average thickness of each layer was about 5 mm, with differences based on the traverse speed. Slower speeds resulted in thicker layers, while faster speeds led to thinner ones. The deposition length for each pass varied between 110 and 120 mm

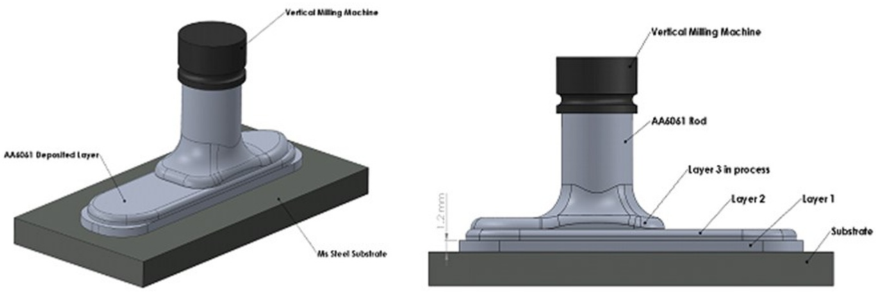

Fig. 2. Schematic diagram of FSD

3.2 Experimental Procedure

The process parameters varied as follows: Feed (Traverse) Rates: 250 mm/min, 300 mm/min, and 350 mm/min

Tool Rotational Speeds (RPM): 900, 1120, and 1400 rpm (applied across layers) so:

- **Sample 1** → Feed 250 mm/min with layer rotations at 900, 1120, and 1400 rpm.
- **Sample 2** → Feed 300 mm/min with layer rotations at 900, 1120, and 1400 rpm.
- **Sample 3** → Feed 350 mm/min with layer rotations at 900, 1120, and 1400 rpm.

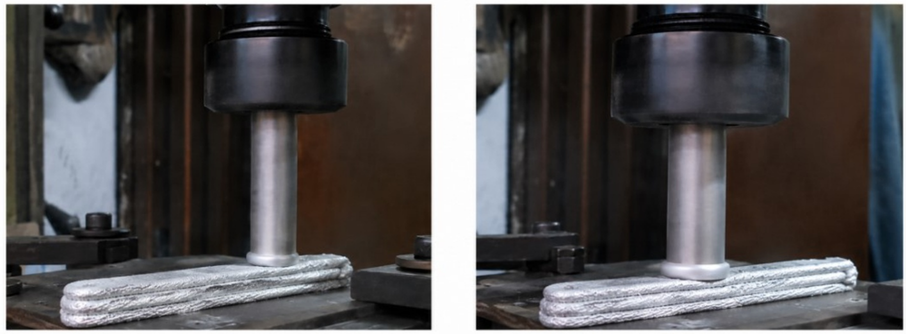

Fig. 3. Additive Friction Stir Deposition of AA6061

The above figure shows the during the deposition, a laser-based infrared heat gun monitored the temperature. The real-time temperature of the workpiece was measured across layers. The observed temperatures showed significant changes. Starting from room temperature (around 32 °C), the material temperature increased to 49 °C, and in later layers reached peak values of about 74 °C and 86 °C. These changes highlighted how feed rate and rotational speed affected the heat input and temperature profile of the build. After deposition, the samples were removed from the mild steel substrate and prepared for further testing. Tensile specimens were taken in the longitudinal direction, while hardness and microstructure samples came from the deposited weld zone. All samples portion were made with a wire EDM machine to ensure precision.

3.3 Material Testing

3.3.1. Tensile Test

Tensile specimens were extracted in the longitudinal direction, while hardness and microstructure samples were taken from the deposited weld zone. All cuts were made using a wire EDM machine to maintain precision. Tensile specimens were prepared according to ASTM E8/E8M-22 standards shown in fig.4 and tested at a displacement speed of 1 mm/min. The geometries of the tensile, hardness, and microstructural samples followed standard guidelines.

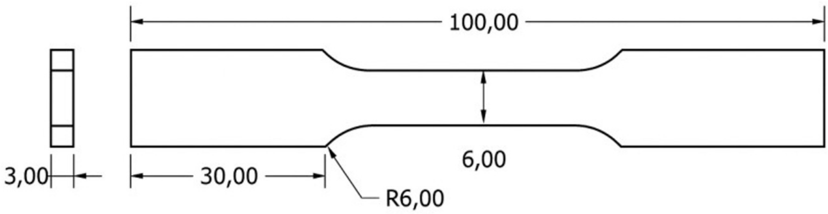

Fig. 4. Tensile Specimen Dimensions (ASTM E8 standard)

Tensile testing was carried out using an Electromechanical Universal Testing Machine (UTM) with a load capacity of 100 KN. The system, manufactured by Hittites India Private Limited (Model: EM-100), is a servo-controlled unit capable of precise displacement control. The dog-bone specimens were obtained through wire-cut EDM and conformed to the standard sub-size dimensions specified by ASTM E8/E8M-22, with a total length of 100 mm, a gauge length of 30 mm, a reduced width of 6 mm, and a thickness of 3 mm fig.4. Testing was performed at a constant crosshead speed of 1 mm/min. The tensile tests provided the ultimate tensile strength (UTS), yield strength (YS), and elongation (%), which serve as critical indicators for comparing the performance of AFSD samples of aluminium alloys. The prepared specimens and their post-fracture conditions fig. 5, confirmed that the methodology was consistent and reliable for evaluating the mechanical behavior of the fabricated deposits. The as-deposited specimens represent the direct outcome of the AFSD process, where microstructural features such as grain refinement, thermal gradients, and potential defects directly influence mechanical behavior. Testing these samples allowed the evaluation of the intrinsic mechanical performance achieved solely through the deposition process.

Following this, the specimens were subjected to a post-deposition heat treatment, after which tensile tests were repeated under the same ASTM E8/E8M-22 conditions. The inclusion of heat-treated samples was crucial because heat treatment helps to relieve residual stresses, homogenize microstructures, and improve mechanical properties such as ductility, yield strength, and hardness. Comparing pre- and post-heat-treatment results enabled us to assess the extent to which heat treatment enhances AFSD-fabricated components and whether the improved performance is competitive with conventional and SLM-produced alloys.

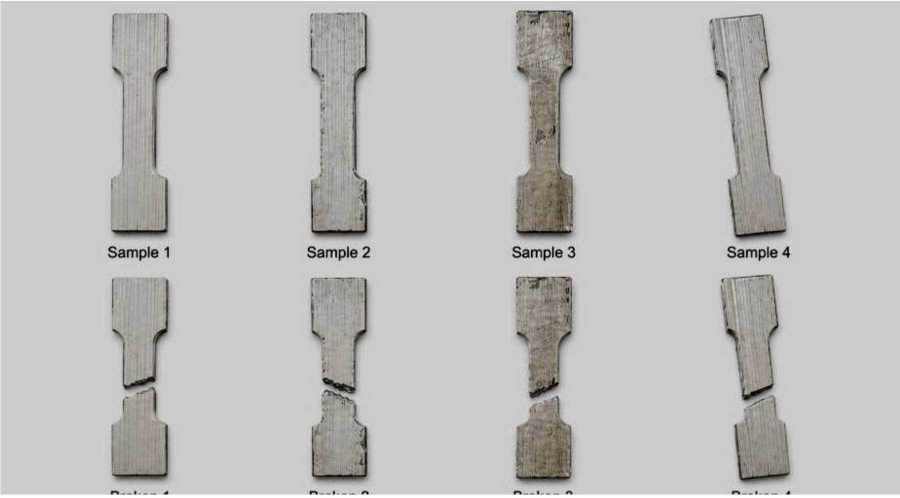

Fig. 5. Tensile specimen before and after fracture of AA6061 by AFSD

3.3.2. Micro hardness Test

The hardness of the AFSD builds was evaluated using the Vickers micro hardness method (HV1.0) in accordance with ASTM E384. Samples were mounted and polished to achieve a mirror finish before indentation. A load of 100 g (HV0.1) with a dwell time of 10–15 seconds was applied using a diamond indenter to create impressions. Measurements were taken at regular intervals along the cross-section of each layer (Layer-1, Layer-2, and Layer-3) to study local hardness variations caused by changes in heat input and plastic deformation during deposition. This procedure was repeated for both the as-deposited and heat-treated conditions shown in below figure.

Fig. 6. Micro hardness samples of AA6061 by AFSD

3.3.3. Pin on Disc Test

The wear behavior of the AFSD samples was studied using a Pin-on-Disc wear testing machine, conforming to the guidelines of ASTM G99. Cylindrical pin specimens (typically 8 mm in diameter and 25 mm in length) were extracted from the deposited blocks using wire EDM to maintain accuracy. The counterface was a hardened EN31 steel disc with a surface hardness of ~60 HRC and a polished finish. Tests were conducted under controlled conditions of normal load, sliding speed, and sliding distance, while the frictional force and coefficient of friction (COF) were continuously monitored using an integrated data acquisition system. Temperature rise at the pin–disc interface was also recorded, providing insights into tribological stability. Wear tests were carried out both before and after heat treatment.

3.3.4. Microstructure Evaluation

Microstructural characterization was performed to evaluate the effect of process parameters and post-deposition heat treatment on grain morphology, bonding quality, and defect distribution within the AFSD builds. Small specimens were carefully extracted from Layer-1, Layer-2, and Layer-3 of each sample to capture variations across the build thickness. Standard metallographic preparation was followed: grinding with SiC papers, polishing with diamond paste, and etching with Kalling's reagent ($CuCl_2$–HCl–ethanol; Kalling's No. 2: 5 g $CuCl_2 \cdot 2H_2O$ + 100 mL concentrated HCl + 100 mL ethanol). Etching was performed at room temperature with short exposure to avoid over-etching, followed by an ethanol rinse and air-drying. Optical microscopy was conducted at 100X and 200X magnifications. The layer-by-layer observation was particularly critical for AFSD because it allowed for assessment of bonding integrity between successive layers, detection of possible defects such as voids or incomplete bonding, and evaluation of grain refinement across interfaces. This also provided insights into how strongly each deposited layer adhered to the previous one, thereby determining the overall structural stability and hardness distribution of the component. Both as-deposited and heat-treated samples were studied to examine changes such as grain boundary recovery, reduction in residual stresses, or possible grain coarsening due to thermal exposure.

From the experimental plan, all three fabricated AFSD samples were subjected to a systematic evaluation of their mechanical properties, including tensile strength, hardness; wear resistance, and microstructural characteristics. Each property was first compared among the three samples to identify the optimal set of process parameters. The best-performing sample was then selected as the representative candidate for further benchmarking. To assess the industrial viability of AFSD, this optimized sample will be compared against conventional aluminium 6061 alloys and SLM-fabricated counterparts. The benchmark values for conventional Al6061-T6 properties are taken from the ASM Handbook: Properties and Selection of Aluminium Alloys [1], which provides widely accepted mechanical data for wrought alloys. For the SLM-processed aluminium alloys, reference values will be obtained from Zhang et al., [6] and Read et al., [7]. Finally, the mechanical property dataset of the best AFSD sample will be compared with literature of SLM and conventional methods. This approach will validate AFSD's competitiveness in real-world applications, establishing a robust foundation for discussion in the subsequent results and analysis section.

4 RESULTS & DISCUSSIONS

4.1 Analysis of Tensile Properties of AA6061 by AFSD Process

Tensile testing was conducted on all three AFSD samples before and after heat treatment to evaluate the effect of thermal processing on mechanical performance.

The results are summarized in terms of ultimate tensile strength (UTS), yield strength (YS), and elongation (%).

Table 1. Before Heat Treatment of AA6061 by ASFD Tensile Samples

Sample	UTS (MPa)	YS (MPa)	Elongation (%)
Sample 1	186.24	137.56	18.72
Sample 2	143.22	102.53	15.68
Sample 3	153.65	121.58	10.32

The tensile properties of the as-deposited AA6061 samples fabricated by Additive Friction Stir Deposition are presented in Table 1. The results indicate that the mechanical response of the deposited samples varied with the processing condition. Sample 1 exhibited the highest ultimate tensile strength of 186.24 MPa and yield strength of 137.56 MPa, along with the maximum elongation of 18.72%. This shows that Sample 1 achieved the most favourable combination of strength and ductility in the as-deposited condition, which may be attributed to better plasticized material flow and stronger interlayer bonding during deposition. Sample 2 showed the lowest UTS and YS values, indicating comparatively weaker strengthening in the deposited region. Sample 3 showed intermediate strength but lower elongation, suggesting reduced ductility. Overall, the results confirm that the AFSD processing condition has a clear influence on the tensile behaviour of AA6061, mainly through its effect on heat input, grain refinement and bonding quality across the deposited layers.

Table 2.Tensile Test of Heat Treatment samples of AA6061 by ASFD

Sample	UTS (MPa)	YS (MPa)	Elongation (%)
Sample 1	242.86	167.5	8.53
Sample 2	140.28	119.25	6.3
Sample 3	178.06	139.1	7.5

The tensile properties of the heat-treated AFSD-AA6061 samples are presented in Table 2. A clear variation in mechanical response was observed among the three samples after heat treatment. Sample 1 exhibited the highest ultimate tensile strength of 242.86 MPa and yield strength of 167.5 MPa, along with an elongation of 8.53%, indicating the best combination of strength and ductility among the tested conditions. This improvement may be attributed to better interlayer consolidation during deposition and the strengthening effect produced by post-deposition heat treatment. In contrast, Sample 2 showed the lowest UTS, YS and elongation values, suggesting a comparatively weaker response to heat treatment. Sample 3 displayed moderate improvement in tensile properties, but its values remained lower than those of Sample 1. The reduction in elongation after heat treatment indicates that the increase in strength occurred at the expense of ductility, which is commonly observed in precipitation-strengthened aluminium alloys. Thus, Sample 1 can be considered the most effective processing condition after heat treatment for achieving improved tensile performance in AFSD-fabricated AA6061.

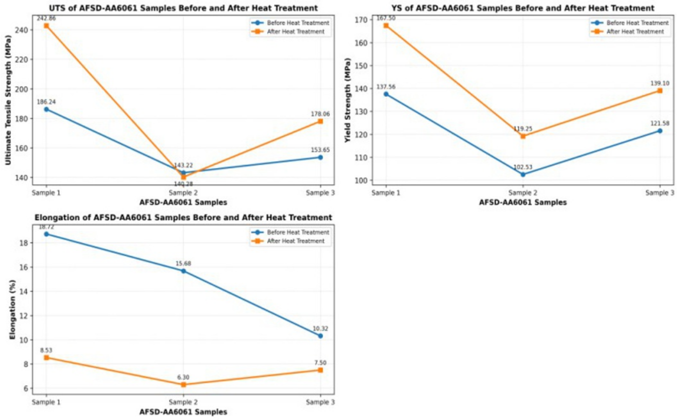

Fig. 7. Variation in ultimate tensile strength, yield strength and elongation of AFSD-AA6061 samples before and after heat treatment

4.2 Analysis of Micro hardness of AA6061 by AFSD Process

To further understand the strengthening effect of friction stir additive manufacturing (AFSD), Vickers microhardness testing was conducted on all three samples both before and after heat treatment. The primary objective was to evaluate how heat treatment influenced the hardness values across different samples and to compare the response of each to thermal processing.

Table 3. Microhardness of AA6061 by AFSD samples before heat treatment

Sample	Reading 1	Reading 2	Reading 3	Average (HV)
S1	115	112	110	112.3
S2	112	116	106	111.3
S3	117	110	111	112.6

Table 4. Microhardness of AA6061 by AFSD samples after heat treatment

Sample	Reading 1	Reading 2	Reading 3	Average (HV)
S1	132	130	135	132.3
S2	135	132	128	131.6
S3	138	146	142	142

Tables 3 and 4 present the Vickers microhardness values of AFSD-fabricated AA6061 samples before and after heat treatment. Three readings were taken for each sample to check the consistency of hardness across the deposited region, and the average hardness value was used for comparison.

Before heat treatment, all three samples showed almost similar hardness values. Sample 1 recorded an average hardness of 112.3 HV, Sample 2 showed 111.3 HV, and Sample 3 showed 112.6 HV. The small difference between the samples indicates that the as-deposited AFSD process produced comparable local resistance to plastic deformation in all three conditions. This may be due to the formation of refined grains during frictional stirring and dynamic recrystallization.

After heat treatment, a clear increase in hardness was observed for all samples. Sample 1 increased from 112.3 HV to 132.3 HV, Sample 2 increased from 111.3 HV to 131.6 HV, and Sample 3 showed the highest improvement, increasing from 112.6 HV to 142 HV. This increase in hardness can be mainly attributed to precipitation strengthening, stress relief and microstructural stabilization during heat treatment.

Among the heat-treated samples, Sample 3 exhibited the highest hardness value of 142 HV. This suggests that Sample 3 responded more strongly to heat treatment compared with the other samples. The higher hardness may be related to a more favourable distribution of strengthening precipitates and local microstructural refinement after thermal exposure.

Overall, the results confirm that heat treatment significantly improved the microhardness of AFSD-AA6061 samples. However, the hardness trend is slightly different from the tensile trend, where Sample 1 showed the best tensile performance. Therefore, Sample 3 can be considered better in terms of hardness, while Sample 1 remains better for overall tensile strength and structural performance.

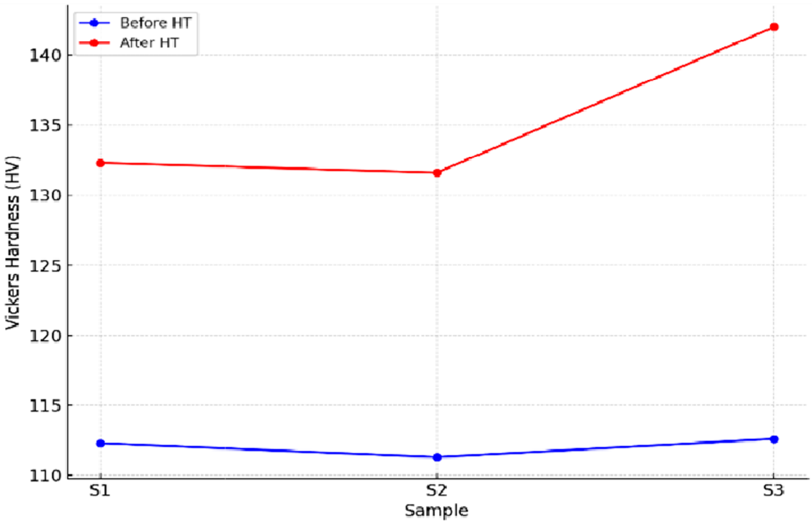

Fig. 8. Variation in average microhardness of AFSD-AA6061 samples before and after heat treatment

4.3 Analysis of Wear Test of AA6061 by AFSD Process

The pin-on-disc test was carried out to evaluate the tribological performance of the AFSD-fabricated samples before and after heat treatment (HT). The parameters analyzed were wear depth (µm), frictional force (N), coefficient of friction (COF), and pin temperature (°C).

Table 5. Wear Rate of AA6061 by AFSD samples before heat treatment

Sample	Avg. Wear (µm)	Avg. Force (N)	Avg. CoF	Avg. Pin Temp (°C)
S1	-0.248	8.02	0.372	43.33
S2	-0.0576	8.849	0.4849	43.44
S3	-0.5162	7.338	0.3234	47.93

Table 6. Wear Rate AA6061 by AFSD samples after heat treatment

Sample	Avg. Wear (µm)	Avg. Force (N)	Avg. CoF	Avg. Pin Temp (°C)
S1	-1.0414	8.227	0.6427	44.19
S2	-1.0867	8.54	0.6854	47.63
S3	-1.539	9.605	0.7461	49.89

Tables 5 and 6 present the tribological behaviour of the AFSD-AA6061 samples before and after heat treatment in terms of average wear, frictional force, coefficient of friction and pin temperature.

Fig.9 Before heat treatment, the three samples showed noticeable differences in wear behaviour. Among them, S2 recorded the lowest wear value at -0.0576 µm, indicating the least material loss under the test conditions, whereas S3 showed the highest wear magnitude at -0.5162 µm. Sample S1 exhibited an intermediate wear value of -0.248 µm. Since the wear values are reported with a negative sign, they may be interpreted as wear depth or downward displacement; therefore, the magnitude of the value is more important than the sign itself. In terms of frictional force, S2 showed the highest value (8.849 N), while S3 showed the lowest (7.338 N). For the coefficient of friction, S2 had the highest CoF (0.4849) and S3 had the lowest (0.3234). The pin temperature before heat treatment was highest for S3 (47.93 °C), suggesting greater frictional heating during sliding.

After heat treatment, all the wear values increased in magnitude. The wear values changed to -1.0414 µm for S1, -1.0867 µm for S2 and -1.539 µm for S3. This indicates that, based on the given data, the samples experienced higher wear loss after heat treatment, with S3 again showing the highest wear magnitude. The average frictional force also increased slightly for S1 and increased more clearly for S3, which reached 9.605 N after heat treatment. Similarly, the coefficient of friction increased in all cases, from 0.372 to 0.6427 for S1, 0.4849 to 0.6854 for S2 and 0.3234 to 0.7461 for S3. The pin temperature also rose after heat treatment, with the highest value again observed for S3 at 49.89 °C.

Overall, the given data suggest that S1 showed the lowest wear magnitude after heat treatment, while S3 showed the poorest wear performance, with the highest wear, highest coefficient of friction and highest pin temperature. The trends in frictional force, coefficient of friction and pin temperature also support this observation. Therefore, based strictly on the tabulated values, S1 may be considered the best-performing sample in terms of wear resistance after heat treatment, whereas S3 appears to be the least wear-resistant condition.

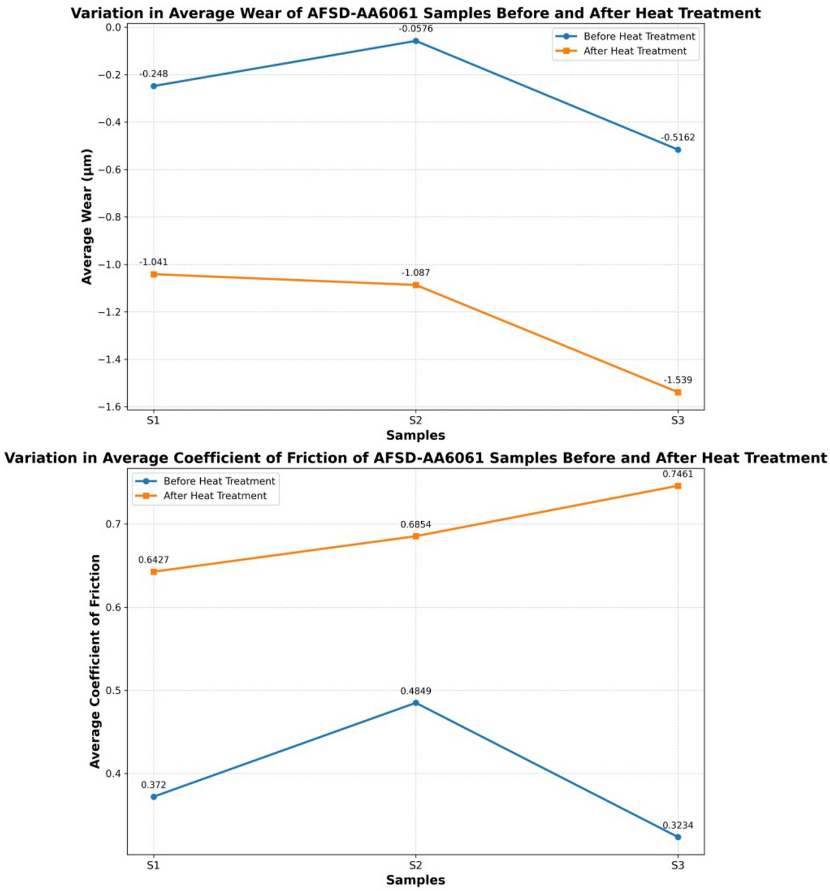

Fig. 9. Variation in Wear rate & average coefficient of friction of AFSD-AA6061 samples before and after heat treatment.

4.4 Analysis of Microstructure of AA6061 by AFSD Process

The Microstructural layered builds produced through Additive friction Stir Deposition manufacturing (AFSD) of AA6061 exhibited the characteristic zones of the process:
The SEM micrographs of AFSD-AA6061 samples before heat treatment are shown in Fig. 10. The as-deposited condition shows clear evidence of material flow, elongated grain structure, fine recrystallized grains and layered flow lines. These features are mainly produced by severe plastic deformation and frictional heating during the AFSD process. The presence of refined equiaxed grains indicates dynamic recrystallization in the stirred region, while aligned grain bands and layered flow lines reveal the direction of plasticized material movement during deposition. Some localized microcrack formation can also be observed, which may be associated with non-uniform bonding or local stress concentration during layer deposition

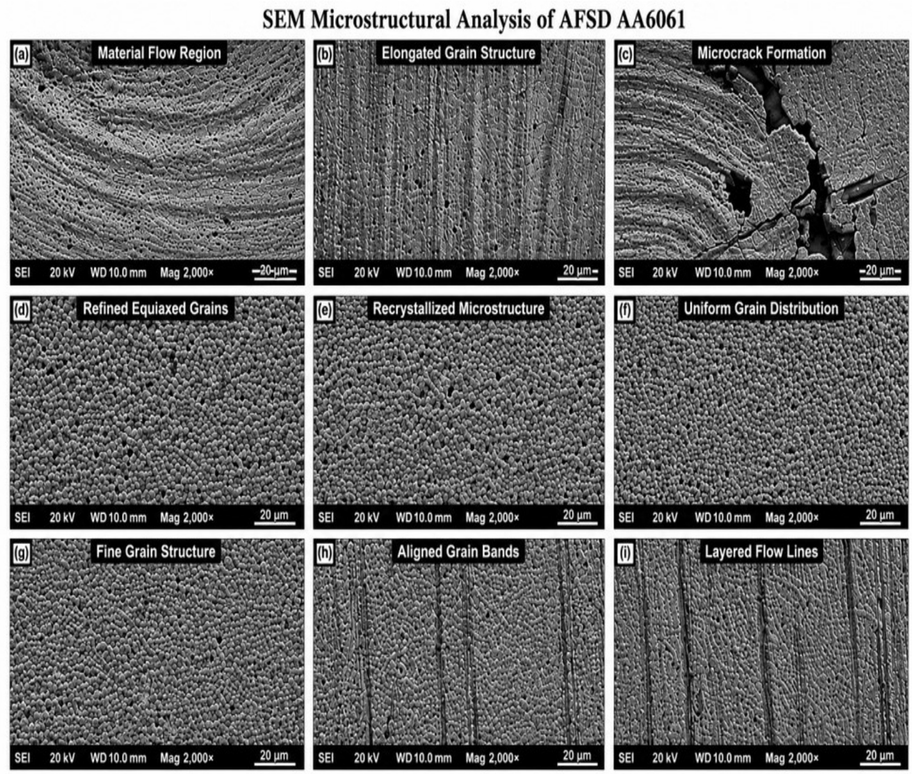

Fig. 10. SEM micrographs of AFSD-AA6061 samples before heat treatment showing flow lines, refined grains and localized microcracks

The SEM micrographs after heat treatment are shown in Fig. 11. Compared with the as-deposited condition, the heat-treated samples show a more homogeneous and stable microstructure. The matrix appears more uniform, with refined recrystallized regions, recovered grain distribution and heat-treated equiaxed structure. The presence of precipitate-modified regions suggests that the heat treatment influenced the distribution of strengthening phases in AA6061. Slight grain coarsening can also be observed in some regions, which is expected due to thermal exposure. Overall, heat treatment reduced the deformation contrast and improved microstructural uniformity, although pre-existing defects or local discontinuities may not be completely eliminated.

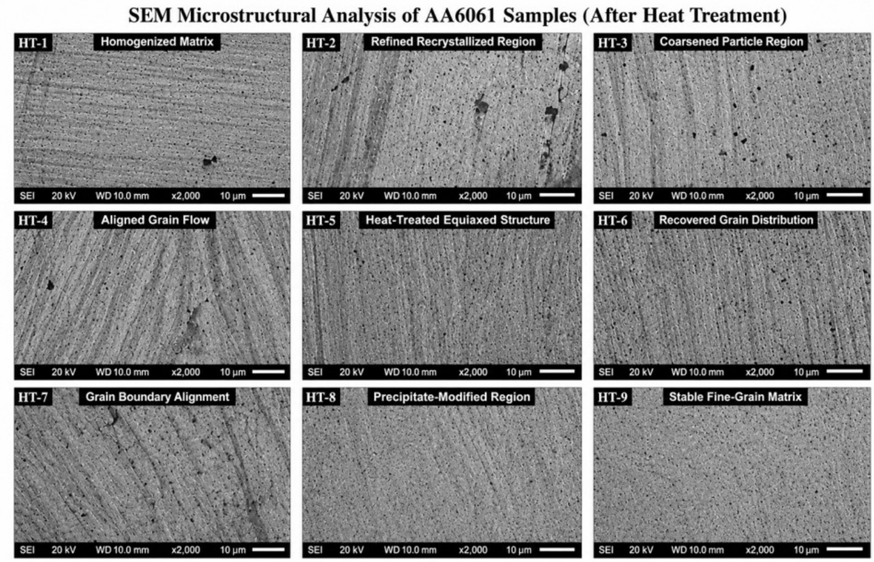

Fig. 11. SEM micrographs of AFSD-AA6061 samples after heat treatment showing flow lines, refined grains and localized microcracks

Table 7. Comparison of microstructural features of AFSD-AA6061 before and after heat treatment

Condition	Overall Average Grain Size, µm	Microstructural Observation
Before Heat Treatment	10.6 µm	Fine dynamically recrystallized grains with visible material flow lines
After Heat Treatment	13.9 µm	Slight grain coarsening with more homogeneous and stable microstructure

5 CONCLUSIONS

The present work focused on the fabrication of AA6061 aluminium alloy using Additive Friction Stir Deposition and studied the changes in mechanical properties and microstructure before and after heat treatment. Based on the experimental results, the following conclusions are made.

- AA6061 was successfully deposited using the AFSD process at different traverse speeds and rotational speeds. The deposited samples showed proper layer formation, which confirms that AFSD is suitable for producing multilayer aluminium alloy deposits.
- Heat treatment improved the tensile strength of the deposited samples. Among all the samples, Sample 1 showed the best tensile performance after heat treatment.

Its ultimate tensile strength increased from 186.24 MPa to 242.86 MPa, showing a clear improvement in strength.

- The yield strength also improved after heat treatment. For Sample 1, the yield strength increased from 137.56 MPa to 167.5 MPa. This indicates that heat treatment helped the material resist plastic deformation more effectively.
- The elongation reduced after heat treatment for all samples. In Sample 1, elongation decreased from 18.72% to 8.53%. This reduction shows the usual trade-off between strength and ductility in heat-treated aluminium alloys.
- The hardness values increased after heat treatment for all samples. Sample 3 showed the highest hardness value of 142 HV after heat treatment. This improvement may be due to precipitation strengthening and microstructural changes caused by the heat-treatment process.
- The microstructure before heat treatment showed fine grains, material flow lines and layer-wise variations. These features were mainly produced due to severe plastic deformation and frictional heating during AFSD.
- After heat treatment, the microstructure became more uniform and stable. The overall average grain size increased from about 10.6 μm before heat treatment to 13.9 μm after heat treatment, showing slight grain growth due to thermal exposure.
- The microstructural changes after heat treatment helped improve strength and hardness. However, any defects or weak bonding regions formed during deposition cannot be completely removed only by heat treatment.
- Based on the overall performance, Sample 1 can be considered the best condition for tensile and structural applications, while Sample 3 is better when higher hardness is required.
- Overall, the study shows that Additive Friction Stir Deposition is a promising solid-state method for fabricating AA6061 components. The process can produce refined microstructures and improved mechanical properties without melting-related defects such as porosity, cracking and solidification problems.

Acknowledgments. The authors acknowledge Mr.Samba Shiva, AMS Material Testing Laboratory, Hyderabad for providing the experimental and material characterization facilities required for this study.The author also express the gratitude to Mr.Morla Nagendram for his valuable cooperation and technical support during this research work

Disclosure of Interests. It is now necessary to declare any competing interests or to specifically state that the authors have no competing interests. Please place the statement with a third level heading in 9-point font size beneath the (optional) acknowledgments[1], for example: The authors have no competing interests to declare that are relevant to the content of this article. Or: Author A has received research grants from Company W. Author B has received a speaker honorarium from Company X and owns stock in Company Y. Author C is a member of committee Z.

---

1 If EquinOCS, our proceedings submission system, is used, then the disclaimer can be provided directly in the system.

References

1. ASM Handbook: Properties and Selection of Aluminum Alloys. (2005). ASM International.
2. Elangovan, K. B. (2008). Influences of tool pin profile and welding speed on the formation of friction stir processing zone in AA6061 aluminum alloy. Materials & Design, 29(2), 362-373.
3. Gao, H. (2025). Microstructure and Properties of 6061 Aluminum Alloy by Additive Friction Stir Deposition. Metals, 15, 539. doi:10.3390/met15050539
4. Gibson, I. R. (2015). Additive Manufacturing Technologies: 3D Printing, Rapid Prototyping, and Direct Digital Manufacturing. Springer.
5. Parameter Optimization for Dissimilar Aluminum Alloys Joined Using Friction Stir Additive Manufacturing: A Screening Study. (2025). Engineering Reports, 7, e13039. doi:10.1002/eng2.13039
6. R.S., M. (2022). Friction stir-based additive manufacturing. Science and Technology of Welding and Joining, 27(3), 141-165. doi:10.1080/13621718.2022.2027663
7. Read, N. (2015). Selective laser melting of AlSi10Mg alloy: Process optimisation and mechanical properties development. Materials & Design, 65, 417-424. doi:10.1016/j.matdes.2014.09.044
8. Zhang, C. (2019). Mechanical behavior and microstructure of AlSi10Mg produced by selective laser melting. Materials Science & Engineering A, 761, 138-150.
9. Khodabakhshi, F., & Gerlich, A. P. (2018). Potentials and strategies of solid-state additive friction-stir manufacturing technology: A critical review. Journal of Manufacturing Processes, 36, 77–92.
10. Yu, H. Z., & Mishra, R. S. (2020). Additive friction stir deposition: A deformation processing route to metal additive manufacturing. Materials Research Letters, 9(1), 71–83.
11. Gopan, V., Wins, K. L. D., & Surendran, A. (2021). Innovative potential of additive friction stir deposition among current laser-based metal additive manufacturing processes: A review. CIRP Journal of Manufacturing Science and Technology, 32, 228–248.
12. Srivastava, A. K., Kumar, N., & Dixit, A. R. (2021). Friction stir additive manufacturing—An innovative tool to enhance mechanical and microstructural properties. Materials Science and Engineering B, 263, 114832.
13. Perry, M. E. J., Griffiths, R. J., Garcia, D., Sietins, J. M., Zhu, Y., & Yu, H. Z. (2020). Morphological and microstructural investigation of the non-planar interface formed in solid-state metal additive manufacturing by additive friction stir deposition. Additive Manufacturing, 35, 101293.
14. Phillips, B. J., Avery, D. Z., Liu, T., Rodriguez, O. L., Mason, C. J., Jordon, J. B., Brewer, L. N., & Allison, P. G. (2019). Microstructure–deformation relationship of additive friction stir-deposited Al–Mg–Si alloy. Materialia, 7, 100387.
15. Zeng, C., Ghadimi, H., Ding, H., Nemati, S., Garbie, A., Rausch, J., & Guo, S. (2022). Microstructure evolution of Al6061 alloy made by additive friction stir deposition. Materials, 15(11), 3676.